Novel Method of Obstacle Avoidance Planning for Redundant Sliding Manipulators

JINGUO LIU[1,2], (Senior Member, IEEE), **YUCHUANG TONG**[1,2,3], (Student Member, IEEE),
ZHAOJIE JU[1,2,4], (Senior Member, IEEE), AND **YUWANG LIU**[1,2], (Member, IEEE)

[1]State Key Laboratory of Robotics, Shenyang Institute of Automation, Chinese Academy of Sciences, Shenyang 110016, China
[2]Institutes for Robotics and Intelligent Manufacturing, Chinese Academy of Sciences, Shenyang 110169, China
[3]University of the Chinese Academy of Sciences, Beijing 100049, China
[4]School of Computing, University of Portsmouth, Portsmouth PO1 3HE, U.K.

Corresponding authors: Jinguo Liu (liujinguo@sia.cn) and Yuwang Liu (liuyuwang@sia.cn)

ABSTRACT In this paper, a weighted additional deviation velocity on the basis of the gradient projection (GP-WADV) method is proposed to solve obstacle avoidance problems of the redundant manipulator under the condition of known end-effector trajectory. The GP-WADV method aims to find the point closest to the obstacle on the link of the manipulator and attach the additional deviation velocity with weighting factors to the point on the basis of the gradient projection method. Utilizing multi-solution characteristics of redundant robots, obstacle avoidance control parameters related to the distance between obstacles and links are proposed according to the gradient projection method for solving inverse kinematic solution. Moreover, a weighted method is adopted to adjust the weighting factors of the primary motion velocity and the additional motion velocity when the link approaches the obstacle, so as to obtain the joint angle solutions more quickly and accurately. The GP-WADV method can ensure that the manipulator can avoid obstacles smoothly without turbulence and solve the highly nonlinear relationship between the position of the manipulator and the joint coordinate, which has the advantages of small amount of calculation, more flexible and convenient real-time control. The advantages of the proposed GP-WADV method are proved by simulation and experiments.

INDEX TERMS Additional deviation velocity method, gradient projection method, obstacle avoidance, redundant manipulator, weighted method.

I. INTRODUCTION

In recent decades, redundant manipulators have played a more and more important role in numerous fields of engineering applications [1]–[4], which possessing more degrees-of-freedom (DOF) in joint space than workspace and offering increased control flexibility for complicated tasks. Redundant design can greatly improve the flexibility of robot manipulators, but may suffer from potential limitations such as system complicity, model uncertainties, physical limitations, which make it challenging to achieve obstacle avoidance [5]–[7]. Obstacle avoidance is a core problem in the control of redundant manipulators, in order to realize human-machine collaboration and integration, manipulators

The associate editor coordinating the review of this manuscript and approving it for publication was Yu-Huei Cheng.

no longer work in a separate environment that is completely isolated, therefore, the obstacle avoidance control is becoming a matter of urgency [8], [9]. However, it remains challenging for manipulators with redundant DOFs, especially when there exist complex physical constraints [10]–[13].

Obstacle modeling and obstacle avoidance of redundant manipulators have been extensively investigated. Traditional obstacle avoidance methods include the free space method based on the C-space method, the artificial potential field method based on the penalty function, the additional deviation velocity method, the gradient projection method and so on. These methods have a few drawbacks, such as inconvenient real-time control, unsuitable environment for random moving obstacles, uncontrollable end-effector path, and uncertainty in the mission process [14], [15]. However, the issue of efficiency and accuracy must be strengthened

while considering the modeling and avoidance of obstacles [31], [32]. Benzaoui *et al.* [11] used the fuzzy adaptive control method to solve the obstacle avoidance problem when the dynamics of the manipulator are uncertain. Korayem *et al.* [16] proposed the application of the Riccati equation controller in the obstacle avoidance of wheeled mobile cooperative robots. Wang *et al.* [17] offered a collision prediction method to estimate the collision parameters in real time. Chen *et al.* [18] developed a minimum acceleration standard scheme for redundant manipulators with obstacle avoidance constraints. Shirafuji *et al.* [19] presented an optimization method to achieve an approximate target trajectory. Lin *et al.* [20] suggested particle swarm optimization to solve the obstacle avoidance problem of redundant manipulators. Zhu *et al.* [33] investigated the control problem of the precise and fast trajectory tracking of free-flight space manipulators. Wei *et al.* [21] recommended an autonomous path planning method of dynamic obstacle avoidance based on the improved rapidly-exploring random trees method. However, due to the large computational costs, those methods can be hardly used online. The application of artificial intelligence methods based on neural networks provides a new idea for manipulator control. These methods are considered to be very promising since its excellent learning ability [22]–[24]. Xu *et al.* [8], [25] propose a novel kinematic controller based on a recurrent neural network (RNN) which is competent in model adaption. Han *et al.* [12] proposed a modern method of dynamic obstacle avoidance on the basis of distance calculation and discrete detection. Xiao *et al.* [26] offered a novel method for avoiding obstacles using the gradient neural network method. Zhang *et al.* [17], [23], [27] established the first adaptive RNN with online learning capabilities for redundant robots with unknown physical parameters. Chen *et al.* [28] used an adaptive projection neural network for the kinematics control of redundant robots with unknown physical parameters. Jin *et al.* [29], [30] performed the path planning of a robot in real time by establishing a dynamic neural network. These methods based on machine learning or numerical iterative methods have the advantage of path smoothing and fast calculation. However, these methods easily fall into local extremum, their iteration time is too long, or the singularity of the robot arm cannot be avoided.

Therefore, in order to solve the above problems, this paper proposed a weighted additional deviation velocity on the basis of the gradient projection (GP-WADV) method to solve obstacle avoidance problems of the redundant manipulator under the condition of known end-effector trajectory. The GP-WADV method aims to find the point closest to the obstacle on the link of the manipulator and attach the additional deviation velocity with weighting factors to the point on the basis of the gradient projection method. Utilizing multi-solution characteristics of redundant robots, obstacle avoidance control parameters related to the distance between obstacles and links are introduced according to the gradient projection method in the equations for solving the inverse kinematic solution. Moreover, a weighted method is adopted

to adjust the weighting factors of the primary motion velocity and the additional motion velocity when the link approaches an obstacle, so as to obtain the joint angles more quickly and accurately. Compared with the traditional gradient projection methods, if the gradient direction is within the constraint range, the traditional method will slow down, however, the GP-WADV method in this paper can quickly calculate the appropriate solution by adjusting the weight parameters. GP-WADV method can ensure that the manipulator can avoid obstacles smoothly without turbulence and solve the highly nonlinear relationship between the position of the robot arm and the joint coordinates, which has the advantages of small amount of calculation, more flexible, more secure and convenient real-time control. Table 1 is comparisons among different methods for obstacle avoidance of redundant manipulators. As shown in Table 1, the GP-WADV method proposed in this paper is more widely used and solves the actual obstacle avoidance problem of redundant manipulators. The advantages of the proposed GP-WADV method are proved by simulation and experiments.

The remainder of this paper is as follows. Section 2 introduces some preliminaries of obstacle avoidance problems and redundant manipulators briefly. Section 3 proposes the improved GP-WADV method to solve obstacle avoidance problems of redundant manipulators under the condition of known end-effector trajectory. In Section 4, the advantages of the proposed GP-WADV method are verified through simulation. In Section 5, the experiment verifies the effectiveness of the GP-WADV method. The research content of the paper is summarized and the future work is presented in Section 6.

II. PRELIMINARIES

This section introduces some preliminaries for obstacle avoidance of redundant manipulators briefly, such as obstacle handling problem, shortest distance from the point to the line segment, concept of the safety zone and kinematic description of redundant manipulators.

A. OBSTACLE HANDLING PROBLEM

Collision detection between the robot and obstacles is the basis for robot motion planning and collision avoidance. The obstacle shape is irregular and sometimes increasingly complicated. To facilitate the research, we conduct simplified processing on the obstacle.

The superposition method is used on the obstacle, which is represented by a sphere envelope. The cylindrical envelope method is applied to represent the robot arm. During calculation, we simplify the manipulator link into the line segment and superimpose the actual link thickness of the manipulator on the obstacle. After the obstacle is processed, the problem of collision between the link and obstacle is reduced to simplify the calculation of the distance from the point (obstacle center or the end-effector of the link) to the line segment (manipulator link), as shown in Fig. 1. Generally, obstacles that are scattered outside the redundant manipulator and do not form a closed path are simplified into

TABLE 1. Comparisons among different methods for obstacle avoidance of redundant manipulators.

| Classification	Methods	Advantages	Disadvantages	Application
This paper	GP-WADV method	This method has the advantages of small amount of calculation, more flexible, more secure and convenient real-time control.	This method needs to calculate the inverse solution of the Jacobian matrix.	Under the condition of known end-effector trajectory
Traditional methods [14], [15]	C-space method, Artificial potential field method based on the penalty function, Additional deviation velocity method, Gradient projection method, Augmented Jacobian method, Weighted least-norm method	These methods have the simple equation structure and can solve simple structures quickly and stably.	These methods are inconvenient for real-time control, are not suitable for random moving obstacles, and have the disadvantages of uncontrollable end-effector path and uncertainty in the mission process. The efficiency and accuracy of these methods need to be strengthened.	Under the condition of simple structure of manipulators and obstacle environment
Modified algorithms	fuzzy adaptive control method [11], Riccati equation controller [16], collision prediction method [17], minimum acceleration standard scheme [18], approximate target trajectory optimization method [19], particle swarm optimization [20], improved rapidly-exploring random trees method [21]	These methods can solve the accuracy and efficiency of traditional methods.	Due to the large computational costs, these methods can be hardly used online.	No requirement for real-time calculation
Artificial intelligence methods based on neural networks [22]–[24]	kinematic controller based on a recurrent neural network (RNN) [8], [25], dynamic obstacle avoidance on the basis of distance calculation and discrete detection [12], gradient neural network [26], adaptive RNN with online learning capabilities [17], [23], [27], adaptive projection neural network [28], dynamic neural network [29], [30]	These methods based on machine learning or numerical iterative methods have the advantage of path smoothing and fast calculation.	These methods easily fall into local extremum, their iteration time is too long, or the singularity of the robot arm cannot be avoided.	No requirement for the end-effector trajectory of manipulators
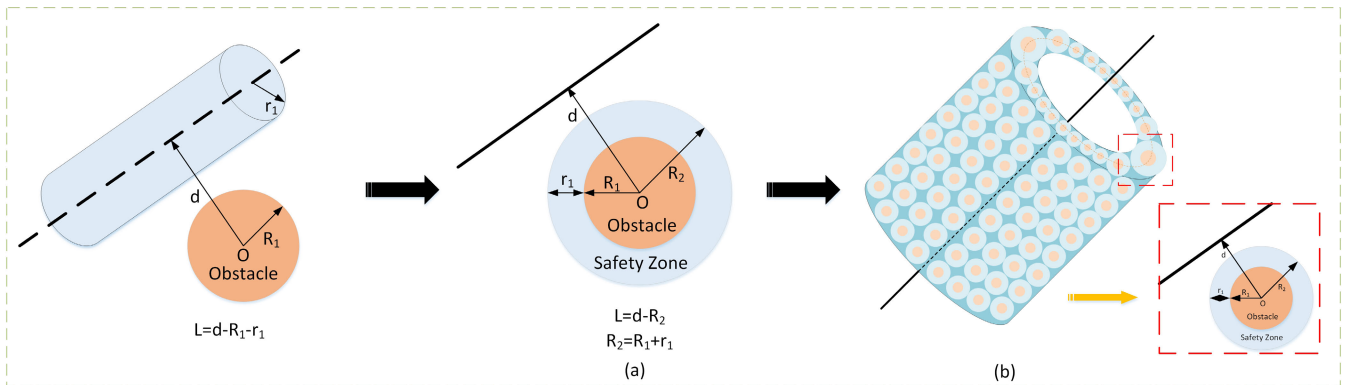
FIGURE 1. (a) Simplified relationship between the manipulator and obstacle, (b) Diagram of the safety zone projection of point P on line segment AB.

corresponding spherical obstacles by the spherical envelope method, as shown in Fig. 1 (a). When the end-effector path of the redundant manipulator passes through a closed gap formed by the obstacles, the method in this paper will be used to model the obstacles as spherical obstacles which are closely spaced arrangement along the edge of this closed gap, as shown in Fig. 1 (b).

B. SHORTEST DISTANCE FROM THE POINT TO THE LINE SEGMENT

The vector method is used to determine the shortest distance between the point P and the line segment AB. By considering

this method, we only need to find the projection of vector $\overrightarrow{AP}$ in the $\overrightarrow{AB}$ direction as follows:

$$\overrightarrow{AC} = \frac{\left(\overrightarrow{AP} \cdot \overrightarrow{AB}\right)}{\left|\overrightarrow{AB}\right|^2}\overrightarrow{AB} = \frac{\left(\overrightarrow{AP} \cdot \overrightarrow{AB}\right)}{\left|\overrightarrow{AB}\right|} \cdot \frac{\overrightarrow{AB}}{\left|\overrightarrow{AB}\right|}, \quad (1)$$

where the new vector $\overrightarrow{AC}$ is the projection vector of $\overrightarrow{AP}$ in the $\overrightarrow{AB}$ direction, and C is the projection point.

Suppose $r = \left(\overrightarrow{AP} \cdot \overrightarrow{AB}\right) / \left|\overrightarrow{AB}\right|^2$. If the situation is similar to that shown in Figs. 2 (a), (b), and (c), then $r \leq 0$, $0 < r < 1$, and $r \geq 1$, respectively. Special cases such as
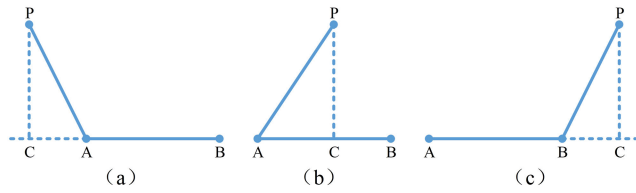
FIGURE 2. Schematic diagram of the position relationship between point P and line segment AB.

the point P on the line segment, the line extension line all apply to the equations.

Therefore, on the basis of the r value, the shortest distance d can be calculated as follows:

$$d = \begin{cases} \left\|\overrightarrow{\mathbf{AP}}\right\| & r \le 0 \\ \left\|\overrightarrow{\mathbf{BP}}\right\| & r \ge 1. \\ \left\|\overrightarrow{\mathbf{CP}}\right\| & 0 < r < 1 \end{cases} \quad (2)$$

C. CONCEPT OF THE SAFETY ZONE

The artificial safety zone is a virtual area surrounding the obstacle, as shown in Fig. 1. A virtual artificial safety zone is defined for each obstacle that can be accessed by the manipulator. The case when the manipulator link enters the safety zone of an obstacle does not mean that the link will collide with the obstacle. However, such case means that the probability of the link colliding with the obstacle increases. When any point in the manipulator enters the safety zone, the obstacle will generate a virtually normal force on the manipulator link to ensure that the link will leave the obstacle along the normal path. When the link leaves the obstacle safety zone, the virtual force disappears.

D. KINEMATIC DESCRIPTION OF REDUNDANT MANIPULATORS

The velocity of the robot task space, that is, the relationship between the operating velocity $\dot{\mathbf{X}} = [x_1, x_2, \cdots, x_m]^{\mathrm{T}}$ and the velocity of the joint space $\dot{\theta} = [\theta_1, \theta_2, \cdots, \theta_n]^{\mathrm{T}}$ is as follows:

$$\dot{\mathbf{X}} = \mathbf{J}\dot{\theta}, \quad (3)$$

where m is defined as the dimension of the task space, n is defined as the dimension of the joint angle space, $\mathbf{J}$ is the Jacobian matrix of the manipulator, $\dot{\mathbf{X}} \in \mathbb{R}^m$, $\dot{\theta} \in \mathbb{R}^n$ and $m \le 6, m \le n$.

For redundant manipulators, i.e., $m < n$, if the rank of the Jacobian matrix is $r = m$, then the column space of the Jacobian matrix is the entire space $\mathbb{R}^m$. For any end-effector velocity $\dot{\mathbf{X}}$, (3) has solutions. Infinite solutions of joint velocities $\dot{\theta}$ exist because the number of equations m is less than the number of unknowns n. Fig. 3 (a) presents the three subspaces when the Jacobian matrix is a full rank.

The self-motion equation of the manipulator is as follows:

$$\mathbf{J}\dot{\theta} = \mathbf{0}. \quad (4)$$

On the basis of linear algebra theory, the general solution $\dot{\theta}$ of a subdeterminate linear equations (4) consists of the particular solutions $\dot{\theta}_s$ and general solutions $\dot{\theta}_h$ of its corresponding homogeneous equations, where $\dot{\theta}_h$ is the nontrivial solution of the system in (4) at time $m < n$, that is, the nonzero solution. All of these solutions constitute the null space of the Jacobian matrix, which is an $n - m$ dimensional subspace of an n dimensional real space $\mathbb{R}^n$, recorded as $\mathbf{N}(\mathbf{J})$. This null space is orthogonal to the row space of the Jacobian matrix, $\mathbb{R}(\mathbf{J}^{\mathrm{T}})$.

From the physical point of view, it can be concluded from the (4) that these motions in the joint space will not cause the motion of the end-effector, and this movement is called self-motion. Since the self-motion will not change the end-effector position and posture of the manipulator, it can satisfy the position and posture of the given task space for the first goal, and change the arrangement of the robot to achieve the second goal of kinematics at the same time, such as obstacles avoidance, singularity and joint limits. Furthermore, redundant manipulators can achieve some dynamic goals such as the most kinetic energy, the most reasonable joint torque distribution, minimum turbulence. In general, the primary goal to realize the trajectory of the robot's end-effector pose is called the primary or first task of the redundant robot, and the motion in the optimized space $\mathbf{N}(\mathbf{J})$ of the performance index of the redundant manipulator is referred to as the secondary task. An important content of the inverse kinematics of a redundant manipulator is to determine its secondary task, i.e., self-motion, in accordance with the requirements of the optimization performance parameters.

When the Jacobian matrix is not a full rank, i.e., $r < m$, the arm is in a singular configuration, and only the end-effector velocity $\dot{\mathbf{X}}$ in the column space $\mathbb{R}(\mathbf{J})$ of the Jacobian matrix has a solution. No solution exists of the end-effector velocity $\dot{\mathbf{X}}$ which is outside the column space $\mathbb{R}(\mathbf{J})$ as well as in the left null space $\mathbf{N}[\mathbf{J}^{\mathrm{T}}]$ of the Jacobian matrix, i.e., the orthogonal complement space $\mathbb{R}(\mathbf{J})$. Fig. 3 (b) displays the four subspaces of the Jacobian matrix that is not a full rank.

III. GP-WADV METHOD

The GP-WADV method aims to find the point closest to the obstacle on the connected robot link and attach the additional deviation velocity with weighting factors to the point on the basis of the gradient projection method. The implementation of the steps will be described in detail below.

A. INVERSE KINEMATICS PROBLEM ON THE BASIS OF GRADIENT PROJECTION METHOD

Inverse kinematics problems of redundant manipulators in this subsection are based on the generalized inverse on the basis of the gradient projection method. Equation (3) indicates the known relationship between the end-effector velocity of the robot and the joint velocity on the basis of linear
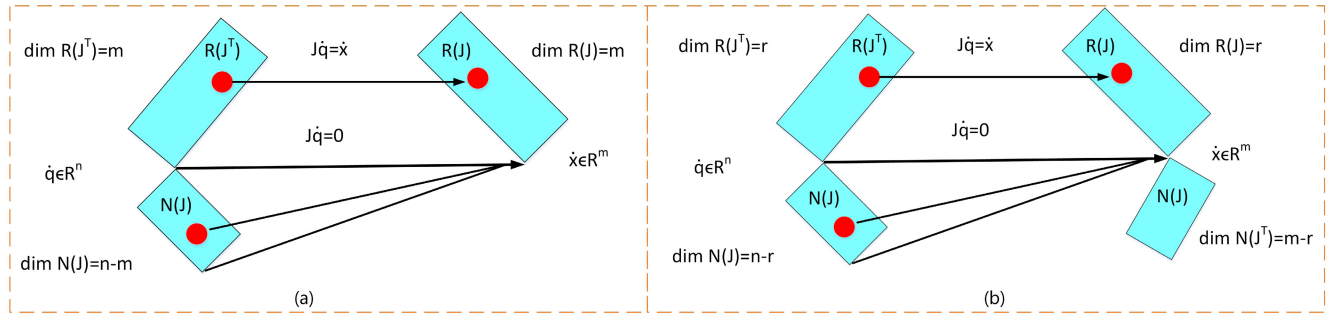
FIGURE 3. Subspace of the Jacobian matrix (a) full rank of Jacobian rows, (b) the rank of the Jacobian matrix is *r*.

algebra theory.

$$\dot{\theta} = \dot{\theta}_s + \dot{\theta}_h = \mathbf{J}^+ \dot{\mathbf{X}} + \left(\mathbf{I} - \mathbf{J}^+ \mathbf{J} \right) \mathbf{v}, \tag{5}$$

where $\mathbf{J}^+$ is the generalized inverse of the Jacobian matrix in the case where $\mathbf{J}$ is a full rank, $\mathbf{J}^+ = \mathbf{J}^{\mathrm{T}} \left(\mathbf{J}\mathbf{J}^{\mathrm{T}} \right)^{-1}$. The first term $\dot{\theta}_s$ of $\dot{\theta}$ is the minimum norm solution of equations $\dot{\mathbf{X}} = \mathbf{J}\dot{\theta}$, which falls in the row space $\mathbb{R}(\mathbf{J}^{\mathrm{T}})$ of the Jacobian matrix, that is, in the *m* dimension subspace of the *n* dimensional real space $\mathbb{R}^n$. The second term $\dot{\theta}_h$ is the general solution of the equations $\mathbf{J}\dot{\theta} = \mathbf{0}$, which is located in the null space $\mathbf{N}(\mathbf{J})$ of the Jacobian matrix. $\dot{\theta}_s$ and $\dot{\theta}_h$ are orthogonal vectors. $\mathbf{v}$ is an arbitrary vector of the *n* dimensional real space $\mathbb{R}^n$, that is, an arbitrary joint velocity vector. $\left(\mathbf{I} - \mathbf{J}^+ \mathbf{J} \right)$ is the null space projection matrix, and $\left(\mathbf{I} - \mathbf{J}^+ \mathbf{J} \right) \mathbf{v}$ is the projection of $\mathbf{v}$ onto the null space $\mathbf{N}(\mathbf{J})$. The second task of the redundant robot is realized by selecting different *v* values. For the convenience of adjustment, $\mathbf{v}$ is usually multiplied by a magnification factor *k* to ensure that (5) becomes:

$$\dot{\theta} = \mathbf{J}^+ \dot{\mathbf{X}} + k \left(\mathbf{I} - \mathbf{J}^+ \mathbf{J} \right) \mathbf{v}. \tag{6}$$

This method on the basis of gradient projection solves the inverse kinematics problem of the redundant manipulator and provides the joint velocity required to satisfy the end-effector motion. According to the gradient projection method, the magnification factor *k* directly affects the velocity of the self-motion of the manipulator, and the large optimization improves its ability to optimize. However, if the magnification factor *k* is too large, then the robot joint velocity will exceed the limit and even make the robot control unstable and cause turbulence in the robot joint motion. Therefore, selecting a reasonable magnification factor *k* is crucial. To facilitate representation, (6) can by simplified to

$$\dot{\theta} = \mathbf{J}^+ \dot{\mathbf{X}} + \mathbf{N}\mathbf{v}, \tag{7}$$

where $\mathbf{N} = k \left(\mathbf{I} - \mathbf{J}^+ \mathbf{J} \right)$.

B. IMPROVED GP-WADV METHOD
When the robot moves in a workspace with obstacles, one or more links may collide with the obstacle. To avoid collisions, a distance threshold $d_{\min}$ should be set. If the distance between the connecting rod and obstacle is greater than $d_{\min}$, then the minimum norm solution $\dot{\theta}_s$ can be directly used.

Otherwise, adjusting the pose of the robot by using the null space vector $\dot{\theta}_h$ on the basis of the gradient projection method is necessary to meet the requirements of obstacle avoidance.

At a certain moment, the distance between the link of the manipulator and the obstacle is less than $d_{\min}$, and the nearest point x_0 between the link and obstacle is called the obstacle avoidance point x_0, as shown in Fig. 4.

To achieve obstacle avoidance, selecting a suitable $\dot{\theta}_h$ is necessary to ensure that the nearest point x_0 has a velocity vector $\dot{\mathbf{X}}_0$ away from the obstacle, which is the additional motion of the redundant robot. The primary and additional motions of the manipulators are expressed as follows:

$$\mathbf{J}\dot{\theta} = \dot{\mathbf{X}}_e, \tag{8}$$
$$\mathbf{J}_0\dot{\theta} = \dot{\mathbf{X}}_0. \tag{9}$$

Equations (8) and (9) represent the primary and additional motions of the manipulator respectively. $\dot{\mathbf{X}}_e$ is the end-effector velocity of the manipulator, $\dot{\mathbf{X}}_0$ is the velocity at which the obstacle avoidance point is set, and $\mathbf{J}_0$ is the Jacobian matrix of the obstacle avoidance point. By substituting (7) into (9), we obtain the following ($\mathbf{v}$ indicates any velocity vector and nonderivative):

$$\mathbf{v} = (\mathbf{J}_0\mathbf{N})^+ \left(\dot{\mathbf{X}}_0 - \mathbf{J}_0\mathbf{J}^+\dot{\mathbf{X}}_e \right). \tag{10}$$

The final solution of $\dot{\theta}$ can be obtained by substituting the above (10) into (5) as follows:

$$\dot{\theta} = \mathbf{J}^+\dot{\mathbf{X}}_e + (\mathbf{J}_0\mathbf{N})^+ \left(\dot{\mathbf{X}}_0 - \mathbf{J}_0\mathbf{J}^+\dot{\mathbf{X}}_e \right). \tag{11}$$

Equation (11) is a kinematic equation of the redundant manipulator considering obstacle avoidance that has clear physical meaning. The first term on the right side of the equation represents the pseudo-inverse solution guaranteeing the velocity $\dot{\mathbf{X}}_e$ of the end-effector or the minimum norm solution, which is the primary task, and the second term represents the DOF satisfying the obstacle avoidance requirement without causing the end-effector to change, which is the additional motion. Among them, velocity $\dot{\mathbf{X}}_0$ of obstacle avoidance is generally determined on the basis of actual environmental information.

In GP-WADV method, $\mathbf{J}_0\mathbf{N}$ depends not only on the position of x_0 but also on the distance vector $\vec{\mathbf{d}}_0$ between x_0 and
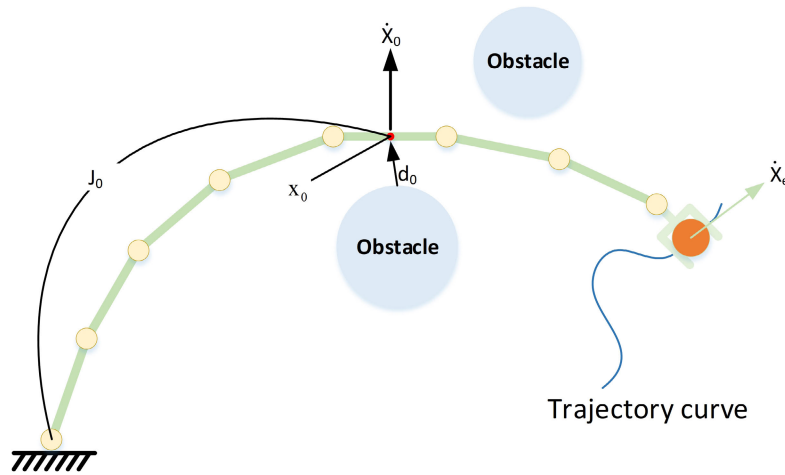
FIGURE 4. Schematic of the obstacle avoidance of the mechanical arm.

the obstacle. Therefore, we consider the direction and use $\mathbf{J}_{\mathbf{d_0}}$ as follows:

$$\mathbf{J}_{\mathbf{d_0}} = \mathbf{n_0}^{\mathrm{T}}\mathbf{J}_0, \tag{12}$$

where $\mathbf{n_0} = \overrightarrow{\mathbf{d_0}}/\left\|\overrightarrow{\mathbf{d_0}}\right\|$ represents the unit vector along direction $\overrightarrow{\mathbf{d_0}}$.

The efficiency of the method is mainly dependent on $\dot{\mathbf{X}}_0$, this value represents the velocity at which the mechanical link escapes from the obstacle when encountering the obstacle as follows:

$$\dot{\mathbf{X}}_0 = \alpha_v \mathbf{v_0}, \tag{13}$$

where α_v is the velocity coefficient and v_0 is the ideal escape velocity because the obstacle will stay away or not react when the arm is inside or outside the safe zone respectively. Hence, d_m is defined as the safety zone radius, α_v is expressed as follows:

$$\alpha_v = \begin{cases} \left(\dfrac{d_m}{\|\overrightarrow{\mathbf{d_0}}\|}\right)^2 - 1 & \left\|\overrightarrow{\mathbf{d_0}}\right\| < d_m \\ 0 & \left\|\overrightarrow{\mathbf{d_0}}\right\| > d_m \end{cases} \tag{14}$$

In order to ensure that the end-effector of the manipulator tracks the desired trajectory and avoid turbulence of the joint velocity. Equation (11) must be appropriately rewritten on the basis of (13) as follows:

$$\dot{\theta} = \mathbf{J}^+\dot{\mathbf{X}}_e + \lambda(d_0)\left(\mathbf{J}_{\mathbf{d_0}}\mathbf{N}\right)^+\left(\dot{\mathbf{X}}_0 - \mathbf{J}_{\mathbf{d_0}}\mathbf{J}^+\dot{\mathbf{X}}_e\right), \tag{15}$$

where $\mathbf{N} = k\left(\mathbf{I} - \mathbf{J}^+\mathbf{J}\right)$, $\dot{\mathbf{X}}_0$ is the unit vector of the obstacle avoidance velocity, α_v is the gain of the obstacle avoidance velocity, and λ is the gain of the homogeneous solution. α_v and λ are functions of distance d_0 of obstacles and collectively referred to as the obstacle avoidance gain. The relationship among the obstacle avoidance gain α_v, homogeneous solution gain λ, and obstacle distance is as shown in Fig. 5.

Assuming that the primary motion and the additional motion are performed simultaneously, the primary task moves
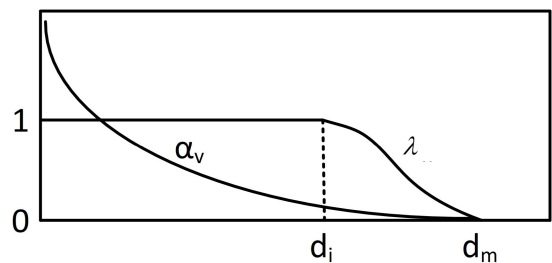

FIGURE 5. Relationship among the obstacle avoidance gain α_v, homogeneous solution gain λ, and obstacle distance.

according to the end-effector trajectory and is constant. When the additional motion is generated on the basis of the distance between the obstacle and the link, it is desirable that the primary task velocity slows down when approaching the obstacle. Hence, the priority of the primary task is reduced, the priority of the additional motion is increased, thereby making the processing transition smoothly. Due to the above basic ideas, this paper designs and introduces the priority adjustment parameter $\lambda(d_0)$ to improve (15), as shown below:

$$\dot{\theta} = (1 - \lambda(\mathbf{d_0}))\mathbf{J}^+\dot{\mathbf{X}}_e$$
$$+ \lambda(\mathbf{d_0})\left(\mathbf{J}_{\mathbf{d_0}}\mathbf{N}\right)^+\left(\dot{\mathbf{X}}_0 - \mathbf{J}_{\mathbf{d_0}}\mathbf{J}^+\dot{\mathbf{X}}_e\right), \tag{16}$$

$$\lambda(\mathbf{d_0}) = \begin{cases} 1 & \|\mathbf{d_0}\| < d_i \\ 1 - \dfrac{1}{2}\left(1 - \cos\left(\pi\dfrac{\|\mathbf{d_0}\| - d_i}{d_m - d_i}\right)\right) & d_i < \|\mathbf{d_0}\| < d_m \\ 0 & d_m < \|\mathbf{d_0}\| \end{cases} \tag{17}$$

where d_i is the distance from the center point of the obstacle to the ith link of the manipulator.
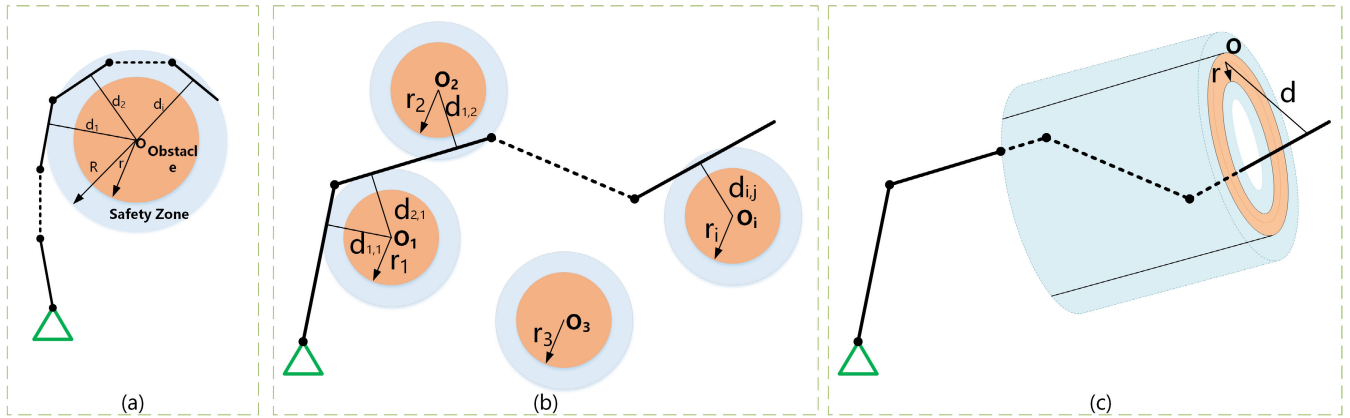
FIGURE 6. Obstacle avoidance relationship diagram for (a) single obstacle, (b)-(c) multiple obstacles.

C. OBSTACLE AVOIDANCE SOLVER

Equation (16) is only applicable to the case wherein a single link enters the safety zone of a single obstacle. When multiple links enter the obstacle safety zone simultaneously, the link closest to the obstacle should be prioritize because the nearest connecting link is the most dangerous and will most likely cause the velocity of the arm to become discontinuous or even cause collision. Fig. 6 (a) shows the obstacle avoidance relationship diagram for a single obstacle.

To consider the other links in the safety zone of obstacles and improve the turbulence in the joint angular velocity caused by the multiple links connecting the obstacle simultaneously, the weighted summation method with weighting factors is used, which is expressed as follows:

$$\dot{\theta} = (1 - \lambda(\mathbf{d_0})_i)\mathbf{J}^+\dot{\mathbf{X}}_e$$
$$+ \sum_{i=1}^{n_0} w_i \lambda(\mathbf{d_0})_i (\mathbf{J_{d_0}N})^+ (\dot{\mathbf{X}}_0 - \mathbf{J_{d_0}J}^+\dot{\mathbf{X}}_e), \quad (18)$$

where n_0 is the number of links entering the obstacle safety zone and w_i and $\lambda(\mathbf{d_0})_i$ are the weight factor and benefit corresponding to the i link entering the obstacle safety zone, respectively. The weighting factor w_i can be expressed as follows:

$$w_i = \frac{d_m - \|\mathbf{d_{0,i}}\|}{\sum\limits_{i=1}^{n_0} (d_m - \|\mathbf{d_{0,i}}\|)}. \quad (19)$$

These factors consider every link that enters the obstacle safety zone to ensure that each link entering the safety zone has a tendency to move away from obstacles. The short distance between the link and obstacle accelerates its velocity of moving away. The closer the shortest distance is, the greater the departure velocity of the link.

Fig. 6 (b) indicates the simultaneous multiple obstacles that are scattered outside the redundant manipulator and do not form a closed path. Meanwhile, Fig. 6 (c) corresponds to the case in Fig. 1 (b) where the end-effector path of the redundant manipulator passes through the closed gap formed

by the obstacles. In these case, multiple obstacles and prioritize the obstacles closest to the connecting link should be considered simultaneously because the nearest obstacle is the most dangerous and may cause the arm velocity to become discontinuous or even collide. Other obstacles within the threshold are also considered. To improve the impact turbulence caused by multiple obstacles on the velocity of the robot arm, the weighted factor summation method is adopted and expressed as follows:

$$\dot{\theta} = (1 - \lambda(\mathbf{d_0})_{i,j})\mathbf{J}^+\dot{\mathbf{X}}_e$$
$$+ \sum_{j=1}^{m_0} \sum_{i=1}^{n_0} w_{i,j} \lambda(\mathbf{d_0})_{i,j} (\mathbf{J_{d_0}N})^+ (\dot{\mathbf{X}}_0 - \mathbf{J_{d_0}J}^+\dot{\mathbf{X}}_e), \quad (20)$$

where m_0 is the number of obstacles in the dangerous state and $w_{i,j}$ and $\lambda(\mathbf{d_0})_{i,j}$ are the weight factor and benefit corresponding to the ith link entering the jth obstacle safety zone, respectively. When the obstacle nearest to the mechanical arm is significantly closer than the other obstacles, the weight factor $w_{i,j}$ is close to 1 or very close to the ideal deviation velocity.

Remark 1: In summary, the steps of the GP-WADV method proposed in the paper are as follows. First, the forward kinematics of the redundant manipulator is solved. Secondly, the collision detection of the links of the manipulator and obstacles is performed on the basis of the results of the forward kinematics solution. During collision detection, the shortest distance between the link and obstacle is calculated, and the assessment of whether the mechanical arm links are in the safe zone is performed. If the manipulator is within the safe zone, then the end-effector of the arm is evaluated if it has reached the target position. In contrast, if the arm is beyond the safe zone, then the joint angles are replanned through the proposed GP-WADV method in this paper and started again from the first step. Finally, if the end-effector of the arm reaches the target position, then the arm can be moved on the basis of the planned joint angles to achieve obstacle avoidance. In contrast, if the manipulator fails to reach the target position, then the pseudo-inverse solution of the arm at

this time is determined, and the process is started again from the first step.

Remark 2: The GP-WADV method performs collision detection between the manipulator and the obstacle in real-time and trajectory detection of the end-effector, and corrects the joint angles in real-time according to the detection results. Therefore, GP-WADV method ensures that the manipulator moves away from obstacles smoothly and achieves obstacle avoidance. In addition, if the manipulator has the need to limit the range of joint angles or avoid kinematic singularities, the GP-WADV method can be used to further attach additional deviation velocity to optimize it to a solution that meets physical constraints.

Remark 3: The GP-WADV method uses the additional deviation velocity method to add additional deviation movement to the main movement during the obstacle avoidance task of the redundant sliding manipulator, and uses the weighting method and gradient projection method to adjust the relationship between the main movement and the additional movement of the redundant sliding manipulator. Combining these methods enables of the redundant sliding manipulator to complete obstacle avoidance tasks faster and more efficiently. Equation (17) and Equation (19) represent the functions between the weight parameters of the GP-WADV method and the minimum distance between the link of the manipulator and the obstacles. It can be concluded from these equations that the principle of GP-WADV method is to calculate the corresponding weight parameters and parameters of the gradient projection method in real time based on the relationship between the safety distance and the shortest distance between the obstacles and the links. Furthermore, in the process of the link of the manipulator approaching the obstacle, the additional velocity deviating from the obstacle is adjusted through the optimization of weighting method and gradient projection method, so that the joint angle of the manipulator can be smoothly transitioned and the redundant sliding manipulator can complete obstacle avoidance tasks smoothly and effectively. In the current research, existing methods mainly include integrating the adaptive algorithm or the self-learning algorithm into the optimization of weight parameters so that the redundant sliding manipulator can adjust the weight parameters online in real time during the obstacle avoidance process. Compared with the method in this paper, the adaptive method and self-learning method combining to the weight parameter optimization require a large number of iterative calculations and easily fall into local extremum. Therefore, the optimization method in this paper is more suitable for real-time control in obstacle avoidance.

IV. SIMULATION

In order to verify the proposed GP-WADV method, this section takes a flat 7-DOF redundant manipulator as an example, and the length of each link is equal to 1 to simulate joint angle, angular velocity, and the minimum distance from

the arm to the obstacle. The simulation results verify the effectiveness and universality of the proposed method.

In the simulation, the parameters include α_v, $w_{i,j}$, $\lambda(\mathbf{d_0})_{i,j}$ and k. The design of these parameters is as follows: parameters α_v, $w_{i,j}$ and $\lambda(\mathbf{d_0})_{i,j}$ are function values obtained from the shortest distance between the obstacle and the link of the manipulator, and the value of k is 6.

A. OBSTACLE AVOIDANCE SIMULATION FOR A SINGLE OBSTACLE

The experiments of Case 1 and Case 2 are aimed at verifying the obstacle avoidance capability of the proposed GP-WADV method when multiple links of the redundant manipulator and the end-effector of the redundant manipulator approach the same obstacle respectively.

1) CASE 1

The initial angle of the manipulator is $\theta_1 = [0.1, 0.1, 0.1, 0.1, 0.1, 0.1, 0.1]rad$. The initial point position is $(6.32, 2.67, 0)$ *mm*. The target point position is $(2.2, 4, 0)$ *mm*.

The obstacle is circular. The central point of the obstacle is set to $(2, 2, 0)mm$, the radius of the obstacle is 1 *mm*, and the radius of the safety zone is 1.5 *mm*. $d_1 = 1$ *mm*, $d_2 = 1.5$ *mm*, $d_3 = 1.5$ *mm*, and $v_0 = 0.5$ *mm/s*. The step size is 0.1 *mm*.

2) CASE 2

The initial angle of the manipulator is $\theta_1 = [2.51, -0.8, -0.8, -0.8, -0.8, -0.8, -0.8]rad$. The initial point position is $(0.85, 0.1, 0)mm$. The target point position is $(4.5, 0, 0)mm$.

The obstacle is circular. The central point of the obstacle is set to $(2.5, -1, 0)mm$, the radius of the obstacle is 1 *mm*, and the radius of the safety zone is 1.5 *mm*. $d_1 = 1$ *mm*, $d_2 = 1.5$ *mm*, $d_3 = 1.5$ *mm*, and $v_0 = 0.5$ *mm/s*. The step size is 0.1 *mm*.

Figs. 7 (a) and (e) shows that the primary tasks both slow down and the priority of the obstacle avoidance motions are both increased when multiple links of redundant manipulator and the end-effector of the redundant manipulator are close to the same obstacle. The distance between each link and obstacle is equal when multiple links are close to the same obstacle. The primary motion and additional motion are superimposed to form a path that crosses the obstacle when the end-effector of the manipulator is close to the obstacle. These features indicate that the weight factors which are generated on the basis of the distance between the obstacle and the link are important for obstacle avoidance. As presented in Figs. 7 (b)-(c) and 7 (f)-(g), the joint angle and angular velocity are within the allowed range when multiple links of the manipulator are close to the obstacle, and the angles and angular velocity are significantly changed when approaching the obstacle. However, there is no obvious mutation phenomenon in these changes, which indicates that the parameters for smoothing priority transition are important. Fig. 7 (d) illustrates that the manipulator link starts to avoid the obstacle and tries to control each manipulator link at the edge of the safety zone when the obstacle is near. As shown
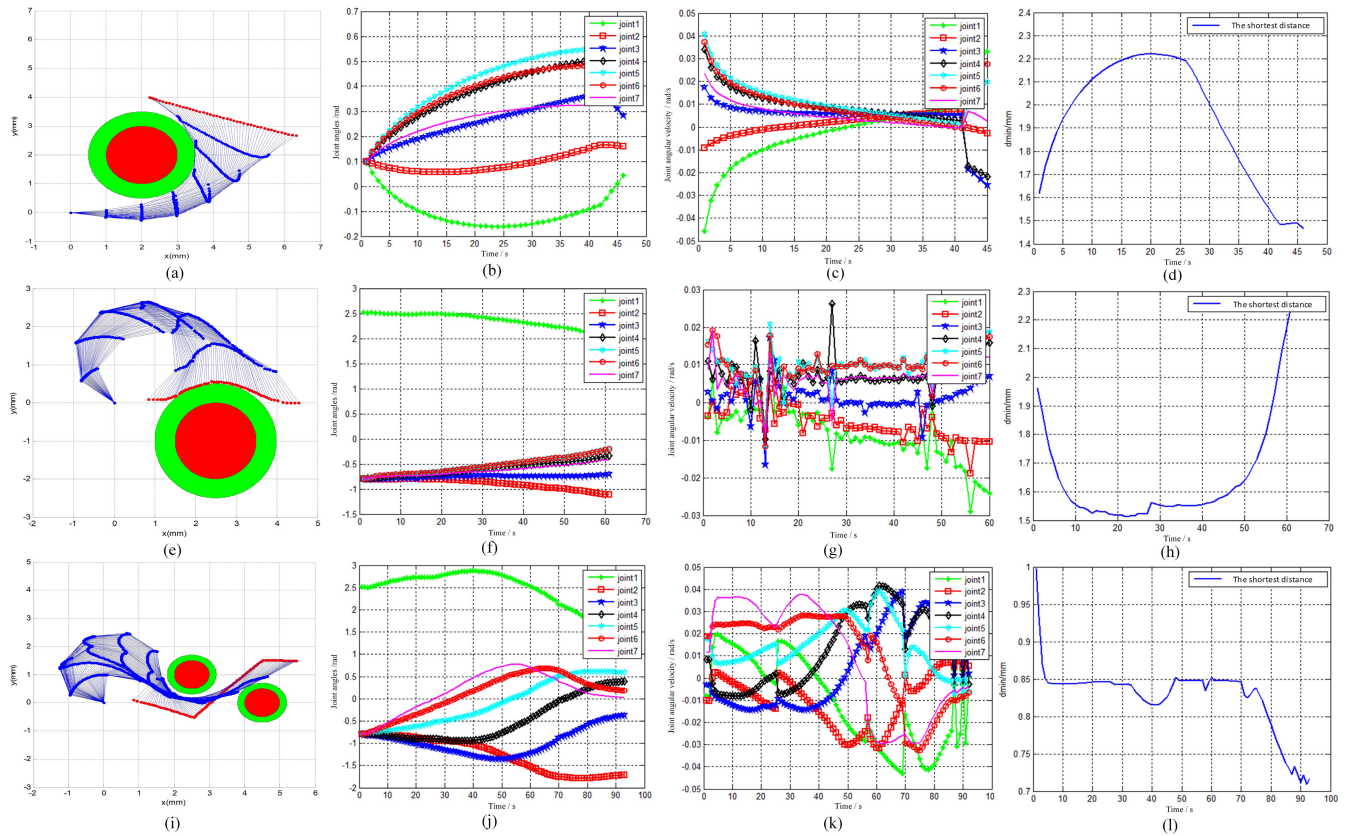
FIGURE 7. Simulation of obstacle avoidance experiment. (a)-(d) Single obstacle: case 1, (e)-(h) Single obstacle: case 2, (i)-(l) Multiple obstacles.

in Fig. 7 (h), when the end-effector of the arm enters the safety zone, it begins to avoid the obstacles and tries to control the end-effector of the arm toward the edge of the safety zone.

B. OBSTACLE AVOIDANCE SIMULATION FOR MULTIPLE OBSTACLES

This subsection aims to verify the obstacle avoidance capability of the GP-WADV method when the multiple links are near to the multiple obstacles.

The initial angle of the manipulator is $\theta_1 = [2.51, -0.8, -0.8, -0.8, -0.8, -0.8, -0.8]rad$. The initial point position is $(0.85, 0.1, 0)mm$. The position of target point 1 is $(2.5, -0.5, 0)mm$. The position of target point 2 is $(4.5, 1.5, 0)mm$. The position of target point 3 is $(5.5, 1.5, 0)mm$.

The obstacle is circular. The central point of the first obstacle is set to $(2.5, 1, 0)mm$, the central point of the second obstacle is set to $(4.5, 0, 0)mm$, the radius of the obstacle is $0.5\ mm$, and the radius of the safety zone is $0.7\ mm$. $d_1 = 0.3\ mm$, $d_2 = 0.3\ mm$, $d_3 = 0.5\ mm$, and $v_0 = 0.5\ mm/s$. The step size is $0.1\ mm$.

Fig. 7 (i) has the same simulation effect as Figs. 7 (a) and (e). The simulation results indicate that the priority of obstacle avoidance based on distance is very important. Figs. 7 (j) and (k) indicate that weight factors which are generated on the basis of the distance between

the obstacles and the links are important for obstacle avoidance. Fig. 7 (l) illustrates that the manipulator starts to avoid the obstacles and tries to control the end-effector of the arm toward the edge of all the safety zones when the links simultaneously enter safety zones of multiple obstacles.

Remark 4: In the obstacle avoidance task of the redundant sliding manipulator, when the minimum distance between the link of the manipulator and the obstacle is smaller than the safety distance, an additional deviation velocity is added to this link. The additional velocity deviates from the obstacle to keep it away from the obstacle, thereby avoiding the obstacle effectively. This paper combines gradient projection method and weighted method for optimization based on the additional deviation velocity method. Therefore, when the links of the manipulator approach the obstacles, the joint angular velocity will be adjusted to ensure that the joint angle of the manipulator does not change abruptly during obstacle avoidance, thereby making the obstacle avoidance process of the redundant sliding manipulator smoother. As presented in Figs. 7 (b)-(c), (f)-(g) and (j)-(k), the joint angular velocity is significantly changed when multiple links of the manipulator are approaching to the obstacle. However, there is no obvious mutation phenomenon in these changes, which indicates that the parameters for smoothing priority transition are important.
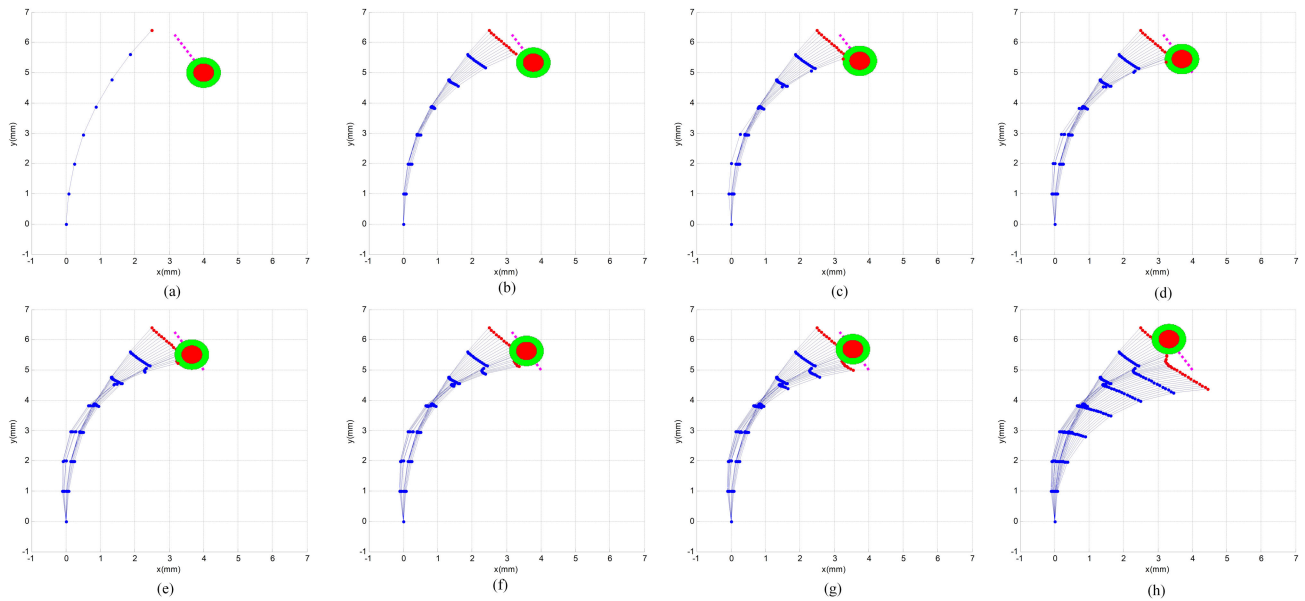
FIGURE 8. Diagram of dynamic changes in the obstacle avoidance of the manipulator.

Remark 5: Furthermore, as we can observe, the angles of joint 1 in Figs. 7 (b), (f) and (j) are quite different from that of other joints in the simulation. The main reasons are as follows: The main idea of the GP-WADV method is to attach the additional deviation velocity to the point closest to the obstacle on the basis of weighting factors and the gradient projection method. In this method, the velocity deviating from the obstacle is added to the calculated minimum norm solution of the position of the end-effector in order to perform the secondary optimization, so that the redundant manipulator can achieve the obstacle avoidance task. Moreover, the research object of this paper is a redundant sliding manipulator, which is not considered the joint angle limitation. Its structural characteristics determine that some of the joint angles in the minimum norm solution of inverse kinematics are different from other joint angles on the basis of no physical constraints, so that the manipulator maintains the advantage of maximum mechanical operation performance during obstacle avoidance tasking. If there is a requirement for joint angle limit, we can take the suitable solution of the inverse kinematics and use the GP-WADV method to further attach additional deviation velocity to optimize it to a solution that meets the physical constraints, thereby solving the obstacle avoidance problem more effectively.

C. MANIPULATOR SIMULATION OF DYNAMIC OBSTACLE AVOIDANCE

This experiment aims to verify the obstacle avoidance capability of the GP-WADV method when the obstacle is a dynamic obstacle.

The accident angles of the mechanical arm are $\theta_1 = [1.5, -0.1, -0.1, -0.1, -0.1, -0.1, -0.1]rad$. The initial point position is $(2.49, 6.39, 0)mm$. The target point position is $(5, 4, 0)mm$.

The obstacle is circular, and the initial position of the obstacle center point is set to $(4, 5, 0)mm$. The last position of the obstacle center point is set to $(3, 6, 0)mm$, the obstacle radius is $0.3\ mm$, and the radius of the safety zone is $0.5\ mm$. $d_1 = 0.3\ mm$, $d_2 = 0.3\ mm$, $d_3 = 0.5\ mm$, and $v_0 = 0.5\ mm/s$. The step size is $0.1\ mm$.

Fig. 8 demonstrates that the effectiveness of the GP-WADV method in the dynamic obstacle. As shown in Figs. 9 (a) and (b), when the end-effector of the arm approaches a dynamic obstacle, the joint angle and angular velocity change within the allowable range. However, there is no obvious mutation phenomenon in these changes, which indicates that the parameters for smoothing priority transition are important. Fig. 9 (c) presents that the arm begins to avoid obstacles and tries to control the end-effector of the arm toward the edge of all the safety zones when it enters the safety zones of the dynamic obstacle.

V. IMPLEMENTATION & VERIFICATION IN THE REDUNDANT SLIDING MANIPULATOR

This section will verify the effectiveness of the proposed GP-WADV method by experimenting with self-developed redundant manipulators through two holes in the box.

A. PLATFORM INTRODUCTION

To investigate the obstacle avoidance performance, this experiment uses the independently developed and designed 7-DOF redundant manipulator on the basis of the linear guide as the research object. Fig. 10 (a) shows the system block diagram of the experimental system of the redundant manipulator. The mechanical system of the arm is mainly composed of a guide rail, a lead screw, a slider, a lumbar joint, and six parallel mechanical arm joints for a total of seven modular joints. This design has the advantages of reconstruction, redundancy, easy assembly, good flexibility, easy
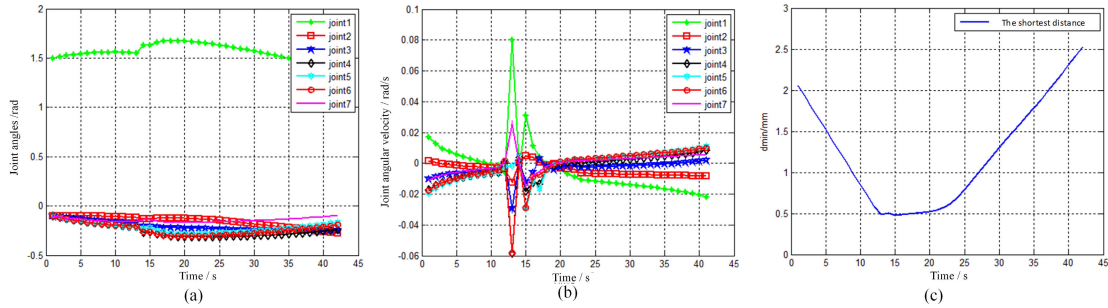
FIGURE 9. Variation diagram of (a) joint angle and (b) joint angular velocity. (c) Minimum distance diagram between the obstacle and the link.
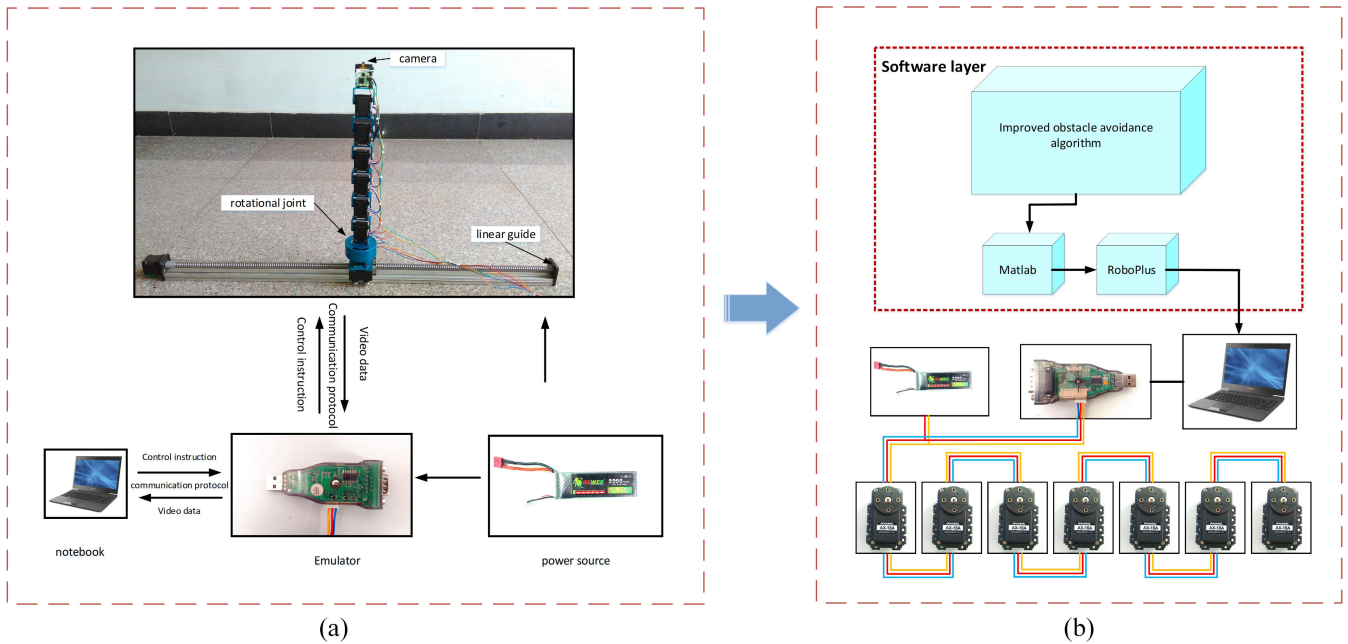

FIGURE 10. (a) Experimental system diagram. (b) Image of the control general structure.

maintenance, wide operating range, and flexible movement. The freedom of the guide can eliminate all blind areas in the operating range. Fig. 10 (b) presents the control system diagram of the experimental platform.

At present, research on obstacle avoidance of redundant sliding manipulator is rare, and redundant sliding manipulators are more conducive to the practical application of the GP-WADV obstacle avoidance method proposed in this paper. Furthermore, the structural characteristics and advantages of the redundant sliding manipulator make it an important innovation and breakthrough in this paper as an experimental platform. In particular, this paper combines the structural characteristics and advantages of the redundant sliding manipulator with the GP-WADV obstacle avoidance method proposed in this paper to achieve obstacle avoidance in a large space. That is to say, during the obstacle avoidance process of the redundant sliding manipulator, the structural features of its sliding guide can be used to perform a large range of motion, and the GP-WADV obstacle

avoidance algorithm is used for the redundant manipulator to achieve obstacle avoidance.

B. IMPLEMENTATION & VERIFICATION EXPERIMENT

The description of the task and the path and the parameter setting are introduced below respectively. The design of the parameters α_v, $w_{i,j}$, $\lambda(d_0)_{i,j}$ and k in the experiment is the same as above.

Task description: The obstacle avoidance task involves passing through two mutually perpendicular holes. The central coordinate of the first hole in the box is $(100, 0, 60)mm$, and the hole radius is $100\ mm$. The central coordinate of the second hole is $(150, 0, 110)mm$, and the hole radius is $100\ mm$. The experimental robot arm will start from the initial configuration, enter through the first hole, and then drill out through the second hole.

Path description: The initial configuration is $[0, -2.82, 0.3, 0.8, 0.8, 0.8, 0.8]rad$, and the corresponding initial position is $(30.33, 0, 140.15)mm$. The positions of targets 1, 2 and 3
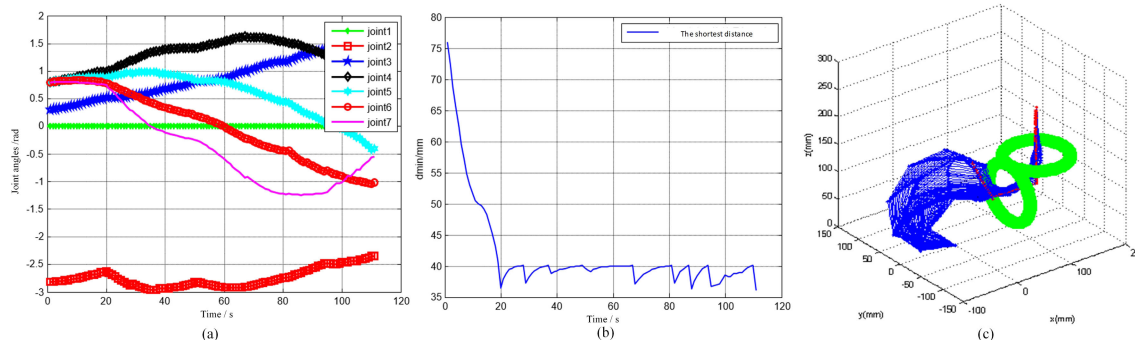
FIGURE 11. Obstacle avoidance experiment. (a) Joint angles. (b) Minimum distance diagram between the obstacle and the links. (c) Simulation results.
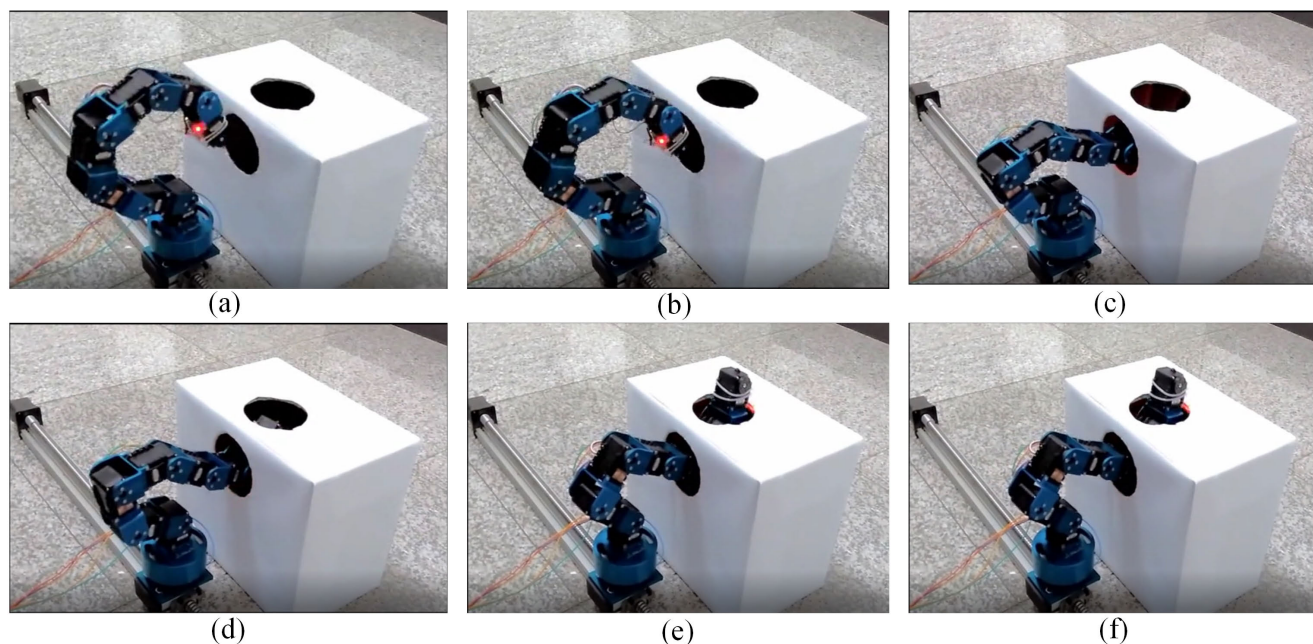

FIGURE 12. Configuration change in the manipulator during obstacle avoidance.

are $(70, 0, 60)mm$, $(150, 0, 60)mm$, and $(150, 0, 200)mm$, respectively, and move along a straight line. The angle unit is radians.

Parameter setting: The radius of the safety zone is 40 mm. $d_1 = 30\ mm$, $d_2 = 40\ mm$, $d_3 = 50\ mm$, and $v_0 = 0.5\ mm/s$. The step size is 5 mm.

As shown in Fig. 11, using the GP-WADV method proposed in this paper can further obtain the change diagram of the joint angles during the obstacle avoidance process, the minimum distance diagram between the obstacle and the link and the process of the obstacle avoidance. As shown in Fig. 11 (a), when multiple links approach the obstacle, the joint angle and angular velocity change within the allowable range. However, there is no obvious mutation phenomenon in these changes, which indicates that the parameters for smoothing priority transition are important. The joint angle of joint 2 is quite different from that of other joints. The main reasons have been analyzed and explained in Section 4, and the GP-WADV method

maintains the maximum operating performance of the manipulator during obstacle avoidance. Fig. 11 (b) demonstrates that each of the links is controlled as far as possible toward the edge of the safety zone when the link is close to the obstacle. Fig. 11 (c) shows that the primary task slows down, the priority of the obstacle avoidance motion increases, and the manipulator smoothly avoids multiple obstacles to reach the final goal when the links are close to multiple obstacles. The smooth transition of this process indicates that the priority of obstacle avoidance based on distance is important.

Fig. 12 presents the configuration change in the manipulator when the manipulator moves within the environment with obstacles. The successful avoidance of obstacles and the attainment of the target position of the manipulator demonstrates the effectiveness of the GP-WADV method. This paper has uploaded video of this process, please see the attached video for details. This experimental system in this paper uses open-loop control, uses Matlab software as a platform to

program and calculate joint angles and joint angular velocity, and then uses Roboplus software to import the calculated data to control the rotation of the motor. Therefore, Figure 11 (a) of this paper shows the joint angle value of the redundant manipulator during obstacle avoidance obtained by programming in Matlab, and the calculated joint angles are imported to control motor, so that the redundant robotic arm can avoid obstacles, as shown in Fig. 12. The AX-18A servo motor used in this experimental platform has reliable quality, stronger torque, faster velocity, stable performance, and high control accuracy. Furthermore, we specifically analyze the main factors that affect the errors of joint angles and end-effector. When the end-effector path is known during the movement of the redundant manipulator, the factor that causes the joint angle error is mainly the rotation error of the motor. The main factor that causes the error of the end-effector is the structural error of the manipulator. Combined with the accuracy standard of the motor and the actual measurement and calculation, the joint angle error is usually within the range of 0.01 *rad*, and the position error is usually within the range of $10^{-7}m$. These errors are so small that they do not affect the completion of obstacle avoidance.

VI. CONCLUSION

This paper proposed a weighted additional deviation velocity on the basis of the gradient projection (GP-WADV) method to solve obstacle avoidance problems of the redundant manipulator under the condition of known end-effector trajectory. The GP-WADV method can ensure that the manipulator can avoid obstacles smoothly without turbulence and solve the highly nonlinear relationship between the position of the robot arm and the joint coordinates, which has the advantages of small amount of calculation, more flexible, more secure and convenient real-time control. The innovation in this study mainly includes the following aspects: (1) The GP-WADV method aims to find the point closest to the obstacle on the link of the manipulator and attach the additional deviation velocity with weighting factors to the point on the basis of the gradient projection method. (2) Obstacle avoidance control parameters related to the distance between obstacles and links are introduced according to the gradient projection method in the equations for solving inverse kinematic solution. (3) The weighted method is adopted to adjust the weighting factors of the primary motion velocity and the additional motion velocity when the link approaches an obstacle, so as to obtain the joint angles more quickly and accurately. (4) The advantages of the proposed GP-WADV method are proved by simulation and experiments.

The proposed method in this study still needs further investigation. Future works can be conducted from the following aspects: obstacle detection sensor or vision sensor can be used for real-time control in an unstructured environment, and dynamic methods can be applied to ensure that the torque remains within the limit during obstacle avoidance for real applications, such as in space [34]–[36].

REFERENCES

[1] H. Cheon and B. K. Kim, "Online bidirectional trajectory planning for mobile robots in state-time space," *IEEE Trans. Ind. Electron.*, vol. 66, no. 6, pp. 4555–4565, Jun. 2019.

[2] S. Li, Y. Zhang, and L. Jin, "Kinematic control of redundant manipulators using neural networks," *IEEE Trans. Neural Netw. Learn. Syst.*, vol. 28, no. 10, pp. 2243–2254, Oct. 2017.

[3] D. Chen, Y. Zhang, and S. Li, "Tracking control of robot manipulators with unknown models: A Jacobian-matrix-adaption method," *IEEE Trans. Ind. Informat.*, vol. 14, no. 7, pp. 3044–3053, Jul. 2018.

[4] L. Jin, S. Li, X. Luo, Y. Li, and B. Qin, "Neural dynamics for cooperative control of redundant robot manipulators," *IEEE Trans. Ind. Informat.*, vol. 14, no. 9, pp. 3812–3821, Sep. 2018.

[5] Z. Mu, W. Xu, and B. Liang, "Avoidance of multiple moving obstacles during active debris removal using a redundant space manipulator," *Int. J. Control, Autom. Syst.*, vol. 15, no. 2, pp. 815–826, Apr. 2017.

[6] W. Xu, J. Zhang, B. Liang, and B. Li, "Singularity analysis and avoidance for robot manipulators with nonspherical wrists," *IEEE Trans. Ind. Electron.*, vol. 63, no. 1, pp. 277–290, Jan. 2016.

[7] K. Ying, T. Qingqing, Z. Ruiyang, and Y. Lv, "A repeatable motion scheme for kinematic control of redundant manipulators," *Comput. Intell. Neurosci.*, vol. 2019, pp. 1–10, Sep. 2019.

[8] Z. Xu, X. Zhou, and S. Li, "Deep recurrent neural networks based obstacle avoidance control for redundant manipulators," *Frontiers Neurorobotics*, vol. 13, Jul. 2019.

[9] D. Guo, F. Xu, L. Yan, Z. Nie, and H. Shao, "A new noise-tolerant obstacle avoidance scheme for motion planning of redundant robot manipulators," *Frontiers Neurorobot.*, vol. 12, p. 51, Aug. 2018.

[10] Y. Zhu, J. Qiao, Y. Zhang, and L. Guo, "High-precision trajectory tracking control for space manipulator with neutral uncertainty and dead-zone nonlinearity," *IEEE Trans. Control Syst. Technol.*, vol. 27, no. 5, pp. 2254–2262, Sep. 2019.

[11] M. Benzaoui, H. Chekireb, M. Tadjine, and A. Boulkroune, "Trajectory tracking with obstacle avoidance of redundant manipulator based on fuzzy inference systems," *Neurocomputing*, vol. 196, pp. 23–30, Jul. 2016.

[12] D. Han, H. Nie, J. Chen, and M. Chen, "Dynamic obstacle avoidance for manipulators using distance calculation and discrete detection," *Robot. Computer-Integrated Manuf.*, vol. 49, pp. 98–104, Feb. 2018.

[13] H. Zhang, H. Jin, Z. Liu, Y. Liu, Y. Zhu, and J. Zhao, "Real-time kinematic control for redundant manipulators in a time-varying environment: Multiple-dynamic obstacle avoidance and fast tracking of a moving object," *IEEE Trans. Ind. Informat.*, vol. 16, no. 1, pp. 28–41, Jan. 2020.

[14] J. Xiang, C. Zhong, and W. Wei, "General-weighted least-norm control for redundant manipulators," *IEEE Trans. Robot.*, vol. 26, no. 4, pp. 660–669, Aug. 2010.

[15] Z. Zhang, L. Zheng, J. Yu, Y. Li, and Z. Yu, "Three recurrent neural networks and three numerical methods for solving a repetitive motion planning scheme of redundant robot manipulators," *IEEE/ASME Trans. Mechatronics*, vol. 22, no. 3, pp. 1423–1434, Jun. 2017.

[16] M. H. Korayem and S. R. Nekoo, "The SDRE control of mobile base cooperative manipulators: Collision free path planning and moving obstacle avoidance," *Robot. Auto. Syst.*, vol. 86, pp. 86–105, Dec. 2016.

[17] Y. Zhang, S. Li, and X. Zhou, "Recurrent-neural-network-based velocity-level redundancy resolution for manipulators subject to a joint acceleration limit," *IEEE Trans. Ind. Electron.*, vol. 66, no. 5, pp. 3573–3582, May 2019.

[18] D. Chen and Y. Zhang, "Minimum jerk norm scheme applied to obstacle avoidance of redundant robot arm with jerk bounded and feedback control," *IET Control Theory Appl.*, vol. 10, no. 15, pp. 1896–1903, Oct. 2016.

[19] S. Shirafuji and J. Ota, "Kinematic synthesis of a serial robotic manipulator by using generalized differential inverse kinematics," *IEEE Trans. Robot.*, vol. 35, no. 4, pp. 1047–1054, Aug. 2019.

[20] C.-J. Lin, T.-H.-S. Li, P.-H. Kuo, and Y.-H. Wang, "Integrated particle swarm optimization algorithm based obstacle avoidance control design for home service robot," *Comput. Electr. Eng.*, vol. 56, pp. 748–762, Nov. 2016.

[21] K. Wei and B. Ren, "A method on dynamic path planning for robotic manipulator autonomous obstacle avoidance based on an improved RRT algorithm," *Sensors*, vol. 18, no. 2, p. 571, 2018.

[22] Z. Mu, T. Liu, W. Xu, Y. Lou, and B. Liang, "A hybrid obstacle-avoidance method of spatial hyper-redundant manipulators for servicing in confined space," *Robotica*, vol. 37, no. 6, pp. 998–1019, Jun. 2019.

[23] Y. Zhang, S. Li, S. Kadry, and B. Liao, "Recurrent neural network for kinematic control of redundant manipulators with periodic input disturbance and physical constraints," *IEEE Trans. Cybern.*, vol. 49, no. 12, pp. 4194–4205, Dec. 2019.

[24] S. Li, M. Zhou, and X. Luo, "Modified primal-dual neural networks for motion control of redundant manipulators with dynamic rejection of harmonic noises," *IEEE Trans. Neural Netw. Learn. Syst.*, vol. 29, no. 10, pp. 4791–4801, Oct. 2018.

[25] Z. Xu, S. Li, X. Zhou, W. Yan, T. Cheng, and D. Huang, "Dynamic neural networks based kinematic control for redundant manipulators with model uncertainties," *Neurocomputing*, vol. 329, pp. 255–266, Feb. 2019.

[26] L. Xiao and Y. Zhang, "Dynamic design, numerical solution and effective verification of acceleration-level obstacle-avoidance scheme for robot manipulators," *Int. J. Syst. Sci.*, vol. 47, no. 4, pp. 932–945, Mar. 2016.

[27] Y. Zhang, S. Chen, S. Li, and Z. Zhang, "Adaptive projection neural network for kinematic control of redundant manipulators with unknown physical parameters," *IEEE Trans. Ind. Electron.*, vol. 65, no. 6, pp. 4909–4920, Jun. 2018.

[28] Y.-J. Chen, M.-Y. Ju, and K.-S. Hwang, "A virtual torque-based approach to kinematic control of redundant manipulators," *IEEE Trans. Ind. Electron.*, vol. 64, no. 2, pp. 1728–1736, Feb. 2017.

[29] L. Jin, S. Li, L. Xiao, R. Lu, and B. Liao, "Cooperative motion generation in a distributed network of redundant robot manipulators with noises," *IEEE Trans. Syst., Man, Cybern. Syst.*, vol. 48, no. 10, pp. 1715–1724, Oct. 2018.

[30] L. Jin, S. Li, H. M. La, and X. Luo, "Manipulability optimization of redundant manipulators using dynamic neural networks," *IEEE Trans. Ind. Electron.*, vol. 64, no. 6, pp. 4710–4720, Jun. 2017.

[31] Z. Jia, X. Qu, S. Chen, N. Zhong, P. Zhang, and F. Ouyang, "Acceleration-level multi-criteria optimization for remedying joint-angle drift of redundant manipulators on complex path tracking," *IEEE Access*, vol. 7, pp. 95716–95724, 2019.

[32] W. Li and R. Xiong, "Dynamical obstacle avoidance of task- constrained mobile manipulation using model predictive control," *IEEE Access*, vol. 7, pp. 88301–88311, 2019.

[33] Y. Zhu, J. Qiao, and L. Guo, "Adaptive sliding mode disturbance observer-based composite control with prescribed performance of space manipulators for target capturing," *IEEE Trans. Ind. Electron.*, vol. 66, no. 3, pp. 1973–1983, Mar. 2019.

[34] X. Zhang, J. Liu, J. Feng, Y. Liu, and Z. Ju, "Effective capture of nongraspable objects for space robots using geometric cage pairs," *IEEE/ASME Trans. Mechatronics*, vol. 25, no. 1, pp. 95–107, Feb. 2020.

[35] X. Zhang, J. G. Liu, Q. Gao, and Z. J. Ju, "Adaptive robust decoupling control of multi-arm space robots using time-delay estimation technique," *Nonlinear Dyn.*, to be published, doi: 10.1007/s11071-020-05615-5.

[36] J. Liu, Y. Tong, Y. Liu, and Y. Liu, "Development of a novel end-effector for an on-orbit robotic refueling mission," *IEEE Access*, vol. 8, pp. 17762–17778, 2020.

from 2016 China Manned Space Academic Conference, and the Outstanding Paper Award from 2017 International Conference on Intelligent Robotics and Applications, and the Best Paper Award from 2018 International Conference on Electrical Machines and systems. He is a Senior Member of the IEEE Technical Committee on Safety, Security, and Rescue Robotics, the IEEE Technical Committee on Marine Robotics, and of Chinese Mechanical Engineering Society. He serves as an Associate Editor or a Technical Editor of several journals, such as the IEEE/ASME Transactions on Mechatronics, *Mechanical Sciences*, *Science China Technological Sciences*, *Chinese Journal of Mechanical Engineering*, and *Chinese Journal of Aeronautics*.

YUCHUANG TONG (Student Member, IEEE) the bachelor's degree in process equipment and control engineering from the Beijing University of Chemical Technology, in 2017. She is currently pursuing the Ph.D. degree in mechatronic engineering from the Shenyang Institute of Automation (SIA), Chinese Academy of Sciences (CAS). Her research interests mainly include manipulator, end-effector, bio-inspired robot, and space robot.

ZHAOJIE JU (Senior Member, IEEE) received the B.S. degree in automatic control and the M.S. degree in intelligent robotics from the Huazhong University of Science and Technology, China, and the Ph.D. degree in intelligent robotics from the University of Portsmouth, U.K.

He held research appointments at University College London, London, U.K., before he started his independent academic position at the University of Portsmouth, in 2012. He has authored or coauthored over 190 publications in journals, book chapters, and conference proceedings and received four best paper awards and one Best AE Award in ICRA2018. His research interests include machine intelligence, pattern recognition and their applications on human motion analysis, multifingered robotic hand control, human–robot interaction and collaboration, and robot skill learning. He is an associate editor of several journals, such as the IEEE Transactions on Cybernetics, the IEEE Transactions on Cognitive and Developmental Systems, and *Neurocomputing*.

JINGUO LIU (Senior Member, IEEE) received the Ph.D. degrees in mechatronics from the Shenyang Institute of Automation (SIA), Chinese Academy of Sciences (CAS), in 2007.

Since January 2011, he has been a Full Professor with SIA, CAS. He has been the assistant director position with the State Key Laboratory of Robotics, since 2008, and has been the associate director position at the Center for Space Automation Technologies and Systems, since 2015. His research interests include bio-inspired robotics and space robot. He has authored/coauthored three books, over 100 articles, and holds 50 patents in above areas. He received the T. J. TARN Best Paper Award in Robotics from the 2005 IEEE International Conference on Robotics and Biomimetics, the Best Paper Award of the Chinese Mechanical Engineering Society, in 2007, the Best Paper Nomination Award from 2008 International Symposium on Intelligent Unmanned Systems, the Best Paper Award

YUWANG LIU (Member, IEEE) received the Ph.D. degree in robotics from the Shenyang Institute of Automation, Chinese Academy of Sciences, in 2010.

He has been working with the SIA, CAS. As a Project Leader or core backbone, he involved in the National Natural Science Foundation of China (NSFC), the National High-Tech R&D Program of China (863 Program), the National Science and Technology Major Project of CNC, and the Key Program of the Chinese Academy of Sciences. He is currently working in robotic mechanism for the application of special environmental science, under-actuated and kinematic coupling mechanism, dexterous operations of robots and multifingered crawling theory, and mechatronics design and precision-driven sensor systems.